

Polarization Bistability of Counterpropagating Laser Beams

Daniel J. Gauthier, Michelle S. Malcuit, Alexander L. Gaeta, and Robert W. Boyd

The Institute of Optics, University of Rochester, Rochester, New York 14627

(Received 13 October 1989)

We have observed bistability in the states of polarization of laser beams counterpropagating through sodium vapor. No external feedback is provided; the beams interact solely through four-wave mixing processes.

PACS numbers: 42.50.Tj, 42.50.Qg, 42.65.Pc

There has been continued interest in optical systems that can possess more than one output state for a given input state. Optical bistability was first proposed theoretically by Szoke *et al.*,¹ observed experimentally by Gibbs, McCall, and Venkatesan,² and has been the subject of extensive theoretical and experimental investigation.³ Most bistable optical devices operate by means of the combined action of nonlinearity and optical feedback, the feedback typically being provided externally by an optical resonator. However, there has been considerable interest in systems that can show optical bistability without the need for external feedback. For example, it has been proposed that reflection at an interface between a linear and nonlinear medium can display optical bistability.⁴ Optical bistability due to mutually induced self-focusing by interacting laser beams has also been predicted.⁵ In addition, recent work has shown that intrinsic optical bistability can occur for a material system in which the absorption increases with increasing degree of excitation.⁶ Also, an early treatment⁷ of four-wave mixing in the standard geometry of optical phase conjugation predicted that the phase-conjugate reflectivity could display bistability and hysteresis for cases in which the four interacting waves have comparable intensities.

In this Letter, we show experimentally that optical bistability can occur due solely to the mutual interaction of two collimated, counterpropagating beams of light. In this case, both the nonlinear coupling and the feedback occur as a result of four-wave mixing processes. We model this interaction theoretically by assuming that the counterpropagating waves interact in an isotropic medium by means of a nonlinear polarization which we express as $P_i = \sum_j \chi_{ij} E_j$, where the field-dependent susceptibility is given by⁸

$$\chi_{ij} = (A - \frac{1}{2}B)(\mathbf{E} \cdot \mathbf{E}^*)\delta_{ij} + \frac{1}{2}B(E_i E_j^* + E_i^* E_j), \quad (1a)$$

where $A = 6\chi_{1122}(-\omega, \omega, \omega, -\omega)$ and $B = 6\chi_{1221}(-\omega, \omega, \omega, -\omega)$. Here $\mathbf{E} = \mathbf{E}_f e^{ikz} + \mathbf{E}_b e^{-ikz}$, where \mathbf{E}_f and \mathbf{E}_b denote the slowly varying complex amplitudes of the forward- and backward-going waves, respectively. Because of the coupling described by Eq. (1a), these field amplitudes obey a reduced wave equation of the form

$$\left[\frac{\partial}{\partial z} \pm \frac{1}{c} \frac{\partial}{\partial t} \right] E_i^{f,b} = \pm 2\pi i k \sum_j [\chi_{ij}^{(0)} E_j^{f,b} + \chi_{ij}^{(\pm 2k)} E_j^{b,f}], \quad (1b)$$

where $\chi_{ij}^{(0)}$ and $\chi_{ij}^{(\pm 2k)}$ denote the dc and $\pm 2k$ spatial Fourier components of χ_{ij} , respectively, and where we take the + (-) sign for the forward (backward) wave. Lytel⁹ and Kaplan and Law¹⁰ have found that the steady-state solution to this set of equations can be multivalued. We have solved Eqs. (1) numerically in order to determine the time dependence of the field amplitudes, and we find that this set of equations can display bistability and hysteresis. An example is shown in Fig. 1, where we treat the case of two beams with linear and nearly parallel input polarizations counterpropagating in

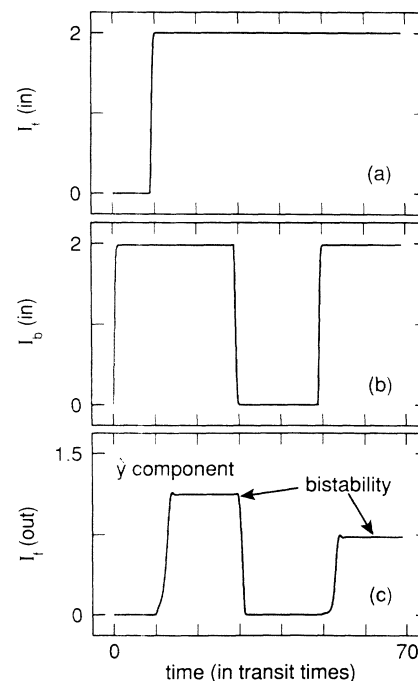


FIG. 1. Prediction of hysteretic bistability in the polarizations of counterpropagating laser beams. (a) The time dependence of the input intensity of the forward-going wave, which is taken to be x polarized. (b) The time dependence of the input intensity of the backward-going wave, which is taken to be linearly polarized at an angle of 0.1 rad with respect to the x axis. (c) The predicted time dependence of the intensity associated with the y component of the transmitted forward-going wave, illustrating bistability. The intensities are plotted in units of $n2\pi ck(A+B/2)L$, where L is the length of the medium.

a nonlinear medium for which the ratio B/A is equal to 1. We similarly find that polarization bistability is predicted for any positive value of the ratio B/A .¹¹ Gaeta *et al.*¹² have shown previously that in some cases the steady-state solution to the set of equations (1) is unstable to the growth of temporal instabilities and that these instabilities can lead to chaotic fluctuations in the states of polarization of the transmitted laser beams. Such chaotic fluctuations were recently observed by ourselves.¹³ However, optical bistability due solely to the mutual interaction of two counterpropagating laser beams has not previously been observed.

The experimental setup we used to observe optical bistability with counterpropagating laser beams is shown schematically in Fig. 2(a). The output of a cw, single-mode ring dye laser with a linewidth of less than 1 MHz is passed through a Faraday isolator and is split into two beams which counterpropagate through a 4-cm-long cell containing sodium vapor. The beams are collimated with diameters of 0.75 mm. Polarizing beam splitters are used to ensure that the beams are linearly polarized with nearly parallel polarizations at the entrance windows of the cell. These beam splitters also analyze the transmitted beams and divert any light generated within the cell in the orthogonal-polarization component into our detection equipment. The sodium-vapor cell is heated by hot flowing oil to a temperature of up to 260°C. We used this procedure to prevent the generation of magnetic fields that would be produced by electrical heating elements. Through use of Helmholtz coils, we canceled the ambient magnetic field to prevent the occurrence of magnetically induced instabilities.¹⁴ All optical components were used at non-normal incidence to prevent external feedback; polarization optical multistability in sodium vapor induced by external feedback has been studied previously.¹⁵ In all cases, the beam intensities were kept well below the threshold for plasma formation to prevent the occurrence of single beam bistability due to this effect.¹⁶

The laser-frequency dependence of the power emitted in the orthogonal-polarization component as the laser frequency is scanned (from low to high frequency) through the D_1 resonance line of sodium is shown in Fig. 2(b) for the case in which each input beam had a power of 46 mW and the atomic number density was $1.6 \times 10^{13} \text{ cm}^{-3}$. The four tick marks indicate the positions of the four hyperfine components of the transition. For the case of the central feature (labeled C) the radiation generated in the orthogonal-polarization component is at the same frequency as the laser. When the laser is tuned to the low-frequency side of resonance (the feature labeled L) the emitted radiation is primarily at the Stokes sideband (i.e., shifted downward from the laser frequency by 1.8 GHz, which is the hyperfine splitting of the electronic ground state); a small amount of radiation is also present at the anti-Stokes and laser frequencies. For the

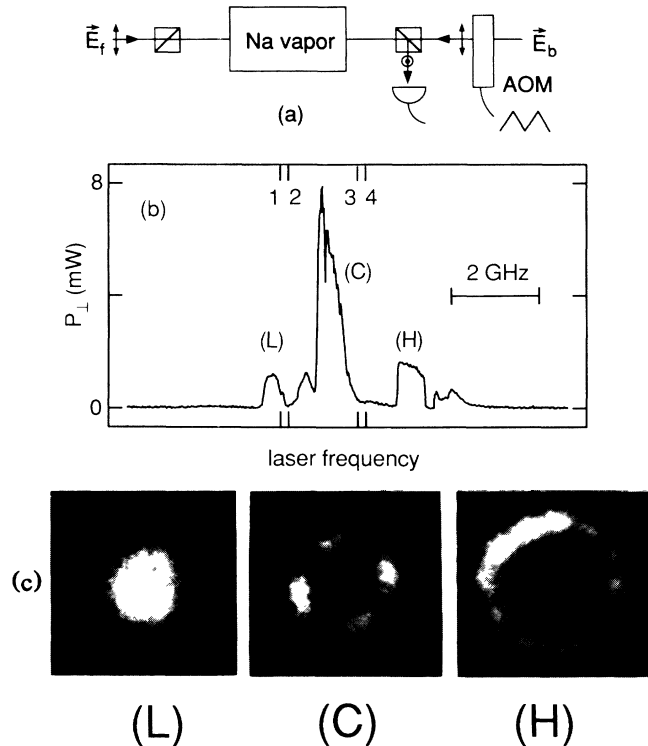


FIG. 2. (a) Experimental setup used to observe cavityless optical bistability in sodium vapor. The power emitted in the polarization component orthogonal to that of the input waves is measured as a function of the power of the backward beam, which is ramped using an acousto-optic modulator (AOM). (b) The time-averaged power of the generated radiation is shown as a function of the laser frequency for a number density of $1.6 \times 10^{13} \text{ atoms cm}^{-3}$, a buffer gas pressure of 15 Torr, and $P_f = P_b = 46 \text{ mW}$. The four tick marks on the horizontal axis, labeled 1-4, indicate the positions of the $(F=2) \rightarrow (F=1)$, $(F=2) \rightarrow (F=2)$, $(F=1) \rightarrow (F=1)$, and $(F=1) \rightarrow (F=2)$ hyperfine components of the $3S_{1/2} \rightarrow 3P_{1/2}$ sodium transition, respectively. (c) The radiation patterns of the light emitted in the orthogonal-polarization component are shown for the low-frequency (L), central-frequency (C), and high-frequency (H) detuning of the laser.

feature at the high-frequency side of resonance (labeled H) most of the emitted radiation is at the anti-Stokes frequency, and a small amount of power is emitted at the Stokes and laser frequencies. These observations demonstrate that significant optical pumping of the ground-state hyperfine levels can occur and that stimulated Raman scattering plays a key role in the nonlinear coupling of the two laser beams.

Figure 2(c) shows the radiation patterns of the emission in the orthogonal-polarization component for each of the features shown in Fig. 2(b). For the case of low-frequency excitation (L) the radiation is emitted on axis, for the case of central excitation (C) the radiation is emitted in a four-lobed structure,¹⁷ and for the case of

high-frequency excitation (H) the radiation is emitted in the form of a cone surrounding the transmitted laser beam. These results show that the four-wave mixing process is influenced by phase-matching effects modified by the nonlinear refractive index of the medium. Conical emission is observed only for the case of detuning to the high-frequency side of resonance; in this case the nonlinear refractive index is positive, which is the condition under which theory predicts that the radiation should be emitted in a cone.¹⁸ The orientation of the radiation pattern for the case of central tuning is observed to drift in a characteristic time of tens of seconds. The surprisingly long time scale of these fluctuations is perhaps due to the long relaxation time of the optically pumped hyperfine levels of the electronic ground state.

We have observed bistability and hysteresis in the polarizations of the transmitted laser beams for both high- and low-frequency detuning of the laser. Figure 3 shows plots of the power P_{\perp} contained in the transmitted forward beam in the polarization component orthogonal to that of the input beams as the power P_b in the backward beam is ramped slowly up and down between 5 and 16 mW. The incident power in the forward beam is held fixed at 74 mW, and the laser is detuned 730 MHz to the high-frequency side of the highest frequency ($F=1 \rightarrow F=2$) hyperfine component of the D_1 transition. In Fig. 3(a), obtained using a number density of $1.6 \times 10^{13} \text{ cm}^{-3}$, the system shows a single hysteresis loop. As the power of the backward beam is increased, the polarization of the forward beam retains its initial state until the power reaches the value of 12.5 mW, at which point the polarization switches abruptly to a different value, leading to the generation of approximately 0.5 mW in the orthogonal polarization. The power P_{\perp} continues to increase as P_b is increased further. When the power P_b is slowly decreased, the system remains on the upper branch until P_b reaches the value 6.5 mW, at which point the polarization of the transmitted forward wave switches abruptly to that of the incident wave. In obtaining this plot, P_b was ramped in a time of 1 msec. We have observed that the shapes of these curves do not change for ramping times as short as 1 μsec or as long as 10 sec. Figure 3(b) shows the behavior for slightly higher atomic number density ($1.9 \times 10^{13} \text{ cm}^{-3}$), where the nonlinear coupling is larger. In this case two stable hysteresis loops are present. Figure 3(c) shows the behavior for the case of a still higher number density of $2.6 \times 10^{13} \text{ cm}^{-3}$. In this case a single hysteresis loop is observed at low intensities, and the system displays dynamic instabilities for intensities higher than 10 mW.

In summary, we have observed bistability and hysteresis in the states of polarization of counterpropagating light waves in a nonlinear medium. Our results are in good qualitative agreement with the theoretical predictions of Kaplan and Law¹⁰ and Gaeta *et al.*¹² These theories model the interaction in terms of a Kerr non-

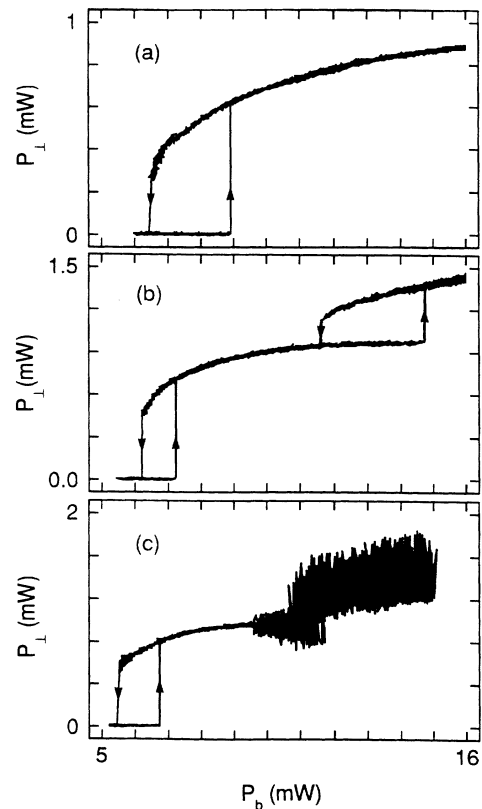


FIG. 3. Power emitted in the forward direction in the polarization component orthogonal to that of the input waves as a function of the backward-wave power, for an atomic number density of (a) $1.6 \times 10^{13} \text{ cm}^{-3}$, (b) $1.9 \times 10^{13} \text{ cm}^{-3}$, and (c) $2.6 \times 10^{13} \text{ cm}^{-3}$.

linearity. To obtain quantitative agreement between theory and experiment, it would be necessary to develop a theoretical model that describes saturation effects and hyperfine optical pumping.

We gratefully acknowledge the financial support of the National Science Foundation, Contract No. ECS 8802761, the Office of Naval Research, and the U.S. Army Research Office University Research Initiative.

¹A. Szoke, V. Daneu, J. Goldhar, and N. A. Kurnit, *Appl. Phys. Lett.* **15**, 376 (1969).

²H. M. Gibbs, S. L. McCall, and T. N. C. Venkatesan, *Phys. Rev. Lett.* **36**, 1135 (1976).

³H. M. Gibbs, *Optical Bistability: Controlling Light with Light* (Academic, Orlando, FL, 1985).

⁴A. E. Kaplan, *Pis'ma Zh. Eksp. Teor. Fiz.* **24**, 132 (1976) [*JETP Lett.* **24**, 114 (1976)].

⁵A. E. Kaplan, *Opt. Lett.* **6**, 360 (1981).

⁶D. A. B. Miller, A. C. Gossard, and W. Wiegmann, *Opt. Lett.* **9**, 162 (1981).

⁷H. G. Winful and J. H. Marburger, *Appl. Phys. Lett.* **36**, 613 (1980).

⁸P. D. Maker and R. W. Terhune, Phys. Rev. **137**, A801 (1965).

⁹R. Lytel, J. Opt. Soc. Am. B **1**, 91 (1984).

¹⁰A. E. Kaplan and C. T. Law, IEEE J. Quantum Electron. **21**, 1529 (1985).

¹¹We do not know what value of the ratio of B/A is most applicable for our experimental conditions, both because of the saturable nature of the nonlinear coupling in a resonantly excited atomic vapor and due to the influences of hyperfine optical pumping of the electronic ground state.

¹²A. L. Gaeta, R. W. Boyd, J. R. Ackerhalt, and P. W. Milonni, Phys. Rev. Lett. **58**, 2432 (1987); A. L. Gaeta, R. W. Boyd, P. W. Milonni, and J. R. Ackerhalt, in *Optical Bistability III*, edited by H. M. Gibbs, P. Mandel, N. Peyghambarian,

and S. D. Smith (Springer-Verlag, New York, 1986), p. 302.

¹³D. J. Gauthier, M. S. Malcuit, and R. W. Boyd, Phys. Rev. Lett. **61**, 1827 (1988).

¹⁴M. Kitano, T. Yabuzaki, and T. Ogawa, Phys. Rev. Lett. **46**, 926 (1981).

¹⁵F. Mitschke, J. Mlynek, and W. Lange, Phys. Rev. Lett. **49**, 1660 (1983).

¹⁶P. Verkerk and G. Grynberg, Europhys. Lett. **6**, 31 (1988).

¹⁷L. A. Lugiato and R. Lefever, Phys. Rev. Lett. **58**, 2209 (1987).

¹⁸G. Grynberg, Opt. Commun. **66**, 321 (1988); W. J. Firth and C. Paré, Opt. Lett. **13**, 1096 (1988); G. Grynberg and J. Paye, Europhys. Lett. **8**, 29 (1989); J. Pender and L. Hesselink, IEEE J. Quantum Electron. **25**, 395 (1989).

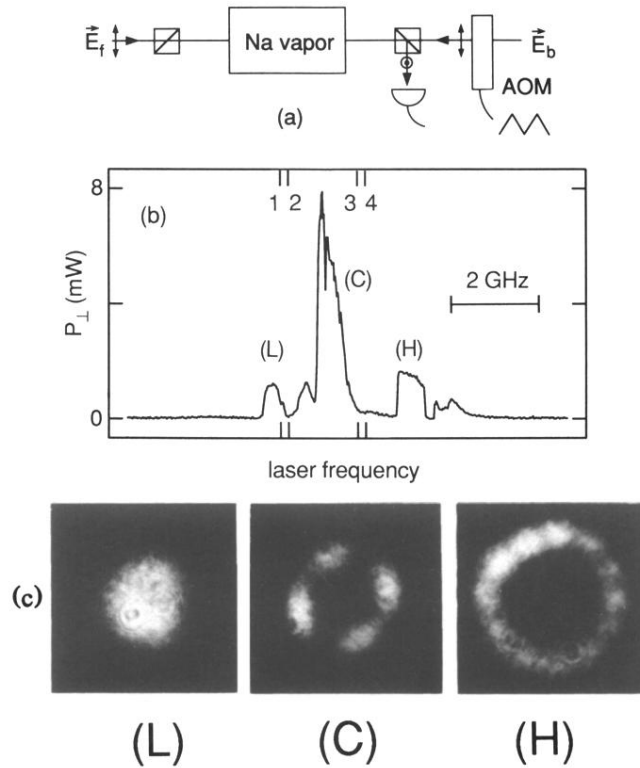


FIG. 2. (a) Experimental setup used to observe cavityless optical bistability in sodium vapor. The power emitted in the polarization component orthogonal to that of the input waves is measured as a function of the power of the backward beam, which is ramped using an acousto-optic modulator (AOM). (b) The time-averaged power of the generated radiation is shown as a function of the laser frequency for a number density of 1.6×10^{13} atoms cm^{-3} , a buffer gas pressure of 15 mTorr, and $P_f = P_b = 46$ mW. The four tick marks on the horizontal axis, labeled 1-4, indicate the positions of the $(F=2) \rightarrow (F=1)$, $(F=2) \rightarrow (F=2)$, $(F=1) \rightarrow (F=1)$, and $(F=1) \rightarrow (F=2)$ hyperfine components of the $3S_{1/2} \rightarrow 3P_{1/2}$ sodium transition, respectively. (c) The radiation patterns of the light emitted in the orthogonal-polarization component are shown for the low-frequency (*L*), central-frequency (*C*), and high-frequency (*H*) detuning of the laser.